Evolution of Spin-Orbital-Lattice Coupling in the RVO$_3$ Perovskites

Peter Horsch,[1] Andrzej M. Oleś,[1,2] Louis Felix Feiner,[3] and Giniyat Khaliullin[1]

[1]*Max-Planck-Institut für Festkörperforschung, Heisenbergstrasse 1, D-70569 Stuttgart, Germany*
[2]*Marian Smoluchowski Institute of Physics, Jagellonian University, Reymonta 4, PL-30059 Kraków, Poland*
[3]*Philips Research Laboratories, High Tech Campus 4, NL-5656 AE Eindhoven, The Netherlands*

We introduce a microscopic model which unravels the physical mechanisms responsible for the observed phase diagram of the RVO$_3$ perovskites. It reveals a nontrivial interplay between superexchange, the orbital-lattice coupling due to the GdFeO$_3$-like rotations of the VO$_6$ octahedra, and orthorhombic lattice distortions. We find that the lattice strain affects the onset of the magnetic and orbital order by partial suppression of orbital fluctuations. The present approach also provides a natural explanation of the observed reduction of magnon energies from LaVO$_3$ to YVO$_3$.

Over the last decade, extensive work on transition metal oxides has demonstrated a strong interrelationship between spin order (SO) and orbital order (OO), often compounded by the occurrence of various types of lattice distortions, resulting in phase behavior of dazzling complexity. Recently, however, impressive experimental work has produced exceptionally detailed information on the phase diagrams of the RMnO$_3$ manganites [1] and the RVO$_3$ vanadates (where $R =$ Lu, Yb, …, La) [2], thus providing a unique challenge to the theory and the opportunity to resolve the interplay between the underlying microscopic mechanisms.

The manganite RMnO$_3$ perovskites exhibit the more common behavior, i.e., upon lowering the temperature, the OO appears first, accompanied by a lattice distortion, at T_{OO}, and thus *modifies* the conditions for the onset of SO at a significantly lower temperature T_N. When the ionic radius r_R of the R^{3+} ions decreases, the Néel temperature T_N gets drastically reduced and the OO transition temperature T_{OO} is enhanced [1]. By contrast, in the RVO$_3$ vanadates the two transitions are close to each other, i.e., $T_{N1} \lesssim T_{\text{OO}}$, the type of order being G-type OO (G-OO) and C-type antiferromagnetic (C-AF), setting in below T_{OO} and T_{N1} [3], respectively [4]. Moreover, whereas T_{N1} again gets reduced for decreasing r_R, T_{OO} exhibits a *nonmonotonic* dependence on r_R [2].

These experimental results demonstrate that spins and orbitals are intimately coupled in the RVO$_3$ vanadates, consistent with the recent observation that these compounds form a unique class characterized by *strong orbital fluctuations* [5–7] which follow from superexchange interactions between almost degenerate t_{2g} orbitals [8,9] and a spin-orbit term [10,11]. Their coupling is also visible in spectacular changes of the SO and OO under pressure [11]. The pressure dependence and thermal conductivity data [12] suggest in turn *strong orbital-lattice coupling* [13]. As in t_{2g} systems Jahn-Teller (JT) interactions are expected to be rather weak, the GdFeO$_3$-like distortions (GFOD)

[14,15] are the prime candidate for being involved in the coupling between orbitals and the lattice.

In this Letter we present a first microscopic approach to the phase diagram of the RVO$_3$ vanadates using an extended spin-orbital model which treats the coupled spin and orbital degrees of freedom in the presence of lattice distortions. We demonstrate that the generic trends observed in the phase diagram of RVO$_3$ can be indeed explained by the theory (see Fig. 1) provided one includes explicitly the coupling between the orbitals and the lattice distortions that increase with decreasing r_R.

A priori, the decreasing ionic radius r_R in the RVO$_3$ perovskites triggers the GFOD obtained by alternating rotations of the VO$_6$ octahedra by an angle ϑ around the b axis, and by an angle φ around the c axis (see inset in
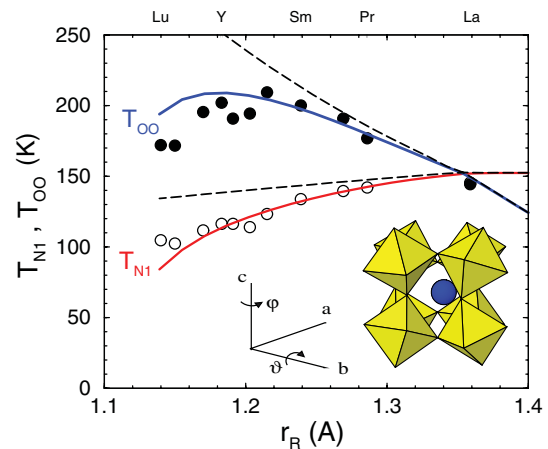

FIG. 1 (color). The orbital transition T_{OO} and Néel T_{N1} temperatures (solid lines) for varying ionic size in RVO$_3$, as obtained from the present theory for the parameter values given in the text, and from experiment (full and empty circles) [2]. Dashed lines indicate T_{OO} and T_{N1} obtained under neglect of orbital-lattice coupling ($g_{\text{eff}} = 0$). The inset shows the GdFeO$_3$-type distortion, with the rotation angles ϑ and φ corresponding to the data of YVO$_3$ [19].

Fig. [1]). This results in a decrease of V-O-V bond angles
(e.g., $\Theta = \pi - 2\vartheta$ along the c direction), and leads to an
orthorhombic distortion $u = (b - a)/a$, where a and b are
the lattice parameters of the *Pbnm* structure. Although
these changes are systematic in the oxides [16], their
relation to the evolution of microscopic parameters and
physical properties such as the onset of OO and SO along
the RVO$_3$ series is not yet fully understood.

The spin-orbital model for RVO$_3$ includes: (i) the super-
exchange interaction [8], (ii) the crystal field (CF) splitting
which follows from the GFOD, (iii) orbital-orbital inter-
actions induced by orbital-lattice coupling, (iv) orbital-
strain coupling. It takes the generic form

$$\mathcal{H} = J \sum_{\langle ij \rangle} \{(\vec{S}_i \cdot \vec{S}_j + S^2)\mathcal{J}_{ij} + \mathcal{K}_{ij}\} - V_c(\vartheta) \sum_{\langle ij \rangle \| c} \tau_i^z \tau_j^z$$
$$+ E_z(\vartheta) \sum_i e^{i\vec{R}_i \vec{Q}} \tau_i^z + V_{ab}(\vartheta) \sum_{\langle ij \rangle \perp c} \tau_i^z \tau_j^z + \mathcal{H}_u, \quad (1)$$

where the parameters $\{E_z, V_{ab}, V_c\}$ depend on the tilting
angle ϑ. The first term describes the superexchange of
strength $J = 4t^2/U$ [here t is the effective $(dd\pi)$ hopping
between t_{2g} orbitals and U the intraorbital Coulomb inter-
action] between V^{3+} ions in the d^2 configuration with $S =$
1 spins. The dependence of J on the rare earth ion R is
weak [1], and is neglected in the present theory; we
adopted $J = 202$ K for the theoretical curves in Fig. [1].
The orbital operators $\mathcal{J}_{ij}$ and $\mathcal{K}_{ij}$ follow from virtual
$d_i^2 d_j^2 \to d_i^3 d_j^1$ charge excitations and depend on Hund's
exchange parameter J_H/U. Their form depends on the
$\langle ij \rangle$-bond orientation; they are given in Ref. [9] for the
actual $(xy)^1(yz/zx)^1$ configuration in cubic vanadates. The
orbital (pseudospin) operators $\tau_i^z \equiv \frac{1}{2}(n_{yz} - n_{zx})_i$ refer to
the two active orbitals: yz and zx [8,9]. The CF splitting of
these two orbitals $\propto E_z$ supports C-type OO [4], with a
modulation vector $\vec{Q} = (\pi, \pi, 0)$ in cubic notation. The
$V_{ab} > 0$ and $V_c > 0$ orbital interactions are due to the JT
and GFOD distortions of the VO$_6$ octahedra, and like E_z
favor C-type OO. Unlike for V_{ab}, it may be expected that
the dependence of V_c on the angle ϑ is weak, and indeed a
constant $V_c(\vartheta) = 0.26J$ reproduces a simultaneous onset
of SO and OO in LaVO$_3$ within the present model [17], i.e.,
$T_{OO} = T_{N1}$; see Fig. [1]. Finally, $\mathcal{H}_u$ describes the coupling
of the orbitals to the orthorhombic distortion u and is
explained below.

To derive the functional dependence of the microscopic
parameters $\{E_z, V_{ab}\}$ on the tilting angle ϑ, we considered
the point charge model, and used the structural data for
RVO$_3$ [18]. Because of the GFOD shown in Fig. [1], the two
active yz/zx orbitals experience the CF splitting E_z. By
considering the ionic charges acting on the t_{2g} orbitals and
analyzing the level splittings, we obtained

$$E_z(\vartheta) = Jv_z \sin^3 \vartheta \cos \vartheta \qquad (2)$$

and verified that the xy orbitals are indeed well below the

$\{yz, zx\}$ orbitals. These qualitative trends are valid in a
range of φ, and for further analysis we adopted a repre-
sentative value $\varphi = \vartheta/2$, similar to the trend in titanates
[15]. It is expected that the angular dependence of the
orbital interaction V_{ab} follows the CF term (2):

$$V_{ab}(\vartheta) = Jv_{ab} \sin^3 \vartheta \cos \vartheta. \qquad (3)$$

An important term in (1), coupling the orbitals to the
lattice, is the one involving the orthorhombic strain u,

$$\mathcal{H}_u \equiv -gu \sum_i \tau_i^x + \frac{1}{2} NK[u - u_0(\vartheta)]^2, \qquad (4)$$

where $g > 0$ is the coupling constant, K is the force con-
stant, and N is the number of V^{3+} ions. In contrast to the
longitudinal field E_z, gu acts as a transverse field; i.e., it
favors that one of the two linear combinations $\frac{1}{\sqrt{2}}(|yz\rangle \pm$
$|zx\rangle)$ is occupied. Since u is a classical variable, we may
minimize Eq. (4) and write the global distortion as
$u(\vartheta; T) \equiv u_0(\vartheta) + (g/K)\langle \tau^x \rangle_T$, consisting of (i) a pure
lattice contribution $u_0(\vartheta)$, and (ii) a contribution due the
orbital polarization $\propto \langle \tau^x \rangle$ which we determined self-
consistently. Both u_0 and $\langle \tau^x \rangle$ are expected to increase
with increasing tilting ϑ. As will be shown below, $\langle \tau^x \rangle$
has only a weak temperature dependence, so we may use

$$g_{\mathrm{eff}}(\vartheta) \equiv gu(\vartheta) = Jv_g \sin^5 \vartheta \cos \vartheta. \qquad (5)$$

Indeed, we shall see below that this strong dependence of
g_{eff} on ϑ is not only necessary to reduce T_{OO} for large
tilting angles ϑ, but is also consistent with the experimen-
tal data for $u(\vartheta)$ [19–22]. Altogether, $\{v_z, v_{ab}, v_g\}$ are the
parameters of the spin-orbital model (1).

In the RMnO$_3$ manganites, mean-field (MF) theory with
classical, on-site, SO and OO parameters can be used to
investigate the phase diagram [23]. However, this approach
with on-site order parameters does not suffice in the vana-
dates [24] when orbital fluctuations stabilizing the C-AF
phase are present [8]—then it becomes essential to deter-
mine self-consistently the orbital singlet correlations
$\langle \vec{\tau}_i \cdot \vec{\tau}_j \rangle$ as well. Hence we used a cluster MF theory for a
bond $\langle ij \rangle$ along the c axis [25], with spin and orbital MF
terms $\langle S^z \rangle$ and $\langle \tau^z \rangle_G \equiv \frac{1}{2} |\langle \tau_i^z - \tau_j^z \rangle|$ which follow from
interactions with the V^{3+} neighbors in all three cubic
directions. Apart from the singlet orbital correlations
$\langle \vec{\tau}_i \cdot \vec{\tau}_j \rangle$, the transverse field $\langle \tau^x \rangle$ was crucial to reproduc-
ing the phase diagram of Fig. [1].

The nontrivial character of the phase diagram and the
underlying spin-orbital coupling in the RVO$_3$ vanadates
can be fully appreciated by analyzing the variation of the
microscopic interactions with decreasing angle Θ (increas-
ing tilting ϑ). While the CF splitting and the orbital
interactions V_{ab} show only a moderate increase for de-
creasing Θ, the orbital polarization g_{eff} increases rapidly
and becomes quite large when $\Theta < 150°$ (Fig. [2]). Note that
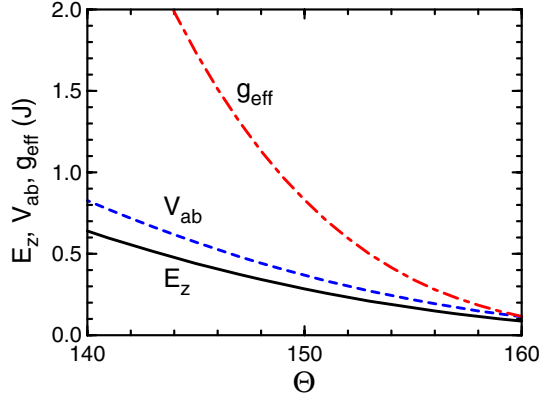the increasing JT term V_{ab} supports the superexchange and

FIG. 2 (color online). Parameters $\{E_z, V_{ab}, g_{\text{eff}}\}$ in Eq. (1) (in units of J) for varying V-O-V bond angle Θ (in degrees). Parameters: $v_z = 17$, $v_{ab} = 22$, $v_g = 740$.

stabilizes the G-OO, both the increasing CF splitting E_z, and the orbital-lattice coupling g_{eff} compete with it.

With the present parameters OO and SO occur simultaneously in LaVO$_3$, and $T_{\text{OO}} = T_{N1} \simeq 0.73J$ (Fig. 3). The orbital polarization $\langle \tau^x \rangle \simeq 0.03$ is here rather weak at T_{N1}, and is further reduced in the ordered phase when the OO parameter $\langle \tau^z \rangle_G$ grows with decreasing $T < T_{\text{OO}}$ (due to finite E_z, the orbitals xz/zy are nonequivalent and $\langle \tau^z \rangle_0 \equiv |\langle \tau_i^z \rangle| > 0$ even for $T > T_{\text{OO}}$ [26]). In contrast, in SmVO$_3$ the OO occurs first at $T_{\text{OO}} \simeq 0.86J$, and the SO follows only at $T_{N1} \simeq 0.65J$. For these parameters the transverse orbital polarization is considerably increased, with $\langle \tau^x \rangle \simeq 0.20$ at T_{N1} (see Fig. 3). Note that the polarization $\langle \tau^x \rangle$ does not change at $T \simeq T_{\text{OO}}$, and only below T_{N1} there is a weak reduction of $\langle \tau^x \rangle$, in agreement with experiment [22]. In both cases the G-OO parameter $\langle \tau^z \rangle_G$ is reduced by singlet orbital fluctuations, being $\langle \tau^z \rangle_G \simeq 0.32$ (0.37) for LaVO$_3$ (SmVO$_3$).

As a result of the competition between the JT term and the CF and orbital-lattice interaction, the temperature T_{OO}

increases first only moderately with decreasing r_R and next *decreases*, resulting in two distinct regimes of the phase diagram of Fig. 1. First, when Θ decreases from 157.4° in LaVO$_3$ to 144.8° in YVO$_3$, increasing V_{ab} dominates and T_{OO} increases (Fig. 1). This is similar to the RMnO$_3$ manganites [1] and can be understood by considering the *total* orbital interactions $K_{ab} \tau_i^z \tau_j^z$ in the ab planes, including both the superexchange J and the JT term V_{ab}; see Fig. 4. Here we use again the ionic radius r_R as in Fig. 1— we deduced its relation to the tilting angle ϑ, $r_R = r_0 - \alpha \sin^2 2\vartheta$ with $r_0 = 1.5$ Å and $\alpha = 0.95$ Å, from the structural data of Refs. [19–22]. Note that the CF splitting E_z increases with decreasing r_R, so it partly compensates for the effect of increasing V_{ab}. Second, the rapidly increasing orbital polarization g_{eff} (Fig. 2) suppresses the tendency towards G-OO and triggers the observed drop of T_{OO} (Fig. 1) when r_R decreases beyond $r_R \sim 1.18$ Å found in YVO$_3$.

The changes in orbital correlations caused by the lattice-induced increase of the total orbital interactions K_{ab} with decreasing r_R (see Fig. 4) suppress the magnetic interactions in the C-AF phase, so the total magnon energy scale $W_{C\text{-AF}} = 4(J_{ab} + |J_c|)$ (at $T = 0$) [9] is reduced from $\sim 1.84J$ in LaVO$_3$ to $\sim 1.05J$ in YVO$_3$, i.e., by a factor close to 1.8. This explains qualitatively the rather small magnon energies observed in the C-AF phase of YVO$_3$ [5]. The reduction is at first instance surprising as the value of J does not change at all, and it is caused solely by the suppression of the singlet orbital correlations $\langle \vec{\tau}_i \cdot \vec{\tau}_j \rangle$ by the transverse field $g_{\text{eff}}(\vartheta)$ (while this effect is small for $g_{\text{eff}} = 0$, in conflict with experiment).

The role played by the orbital-strain coupling (4) in the phase diagram of the RVO$_3$ compounds becomes even more transparent by comparing the dependence of g_{eff} on the ionic radius r_R with the actual lattice distortion u in RVO$_3$ (Fig. 5). Surprisingly, we find that the experimental
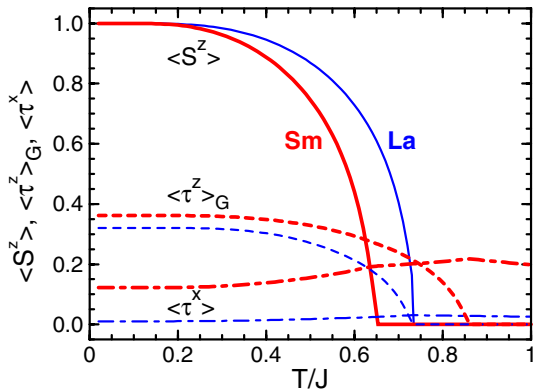

FIG. 3 (color online). Spin $\langle S^z \rangle$ (solid lines) and G-type orbital $\langle \tau^z \rangle_G$ (dashed lines) order parameters, vanishing at T_{OO} and T_{N1}, respectively, and the transverse orbital polarization $\langle \tau^x \rangle$ (dash-dotted lines) for LaVO$_3$ and SmVO$_3$ (thin and heavy lines) for $V_c = 0.26J$; other parameters as in Fig. 2.
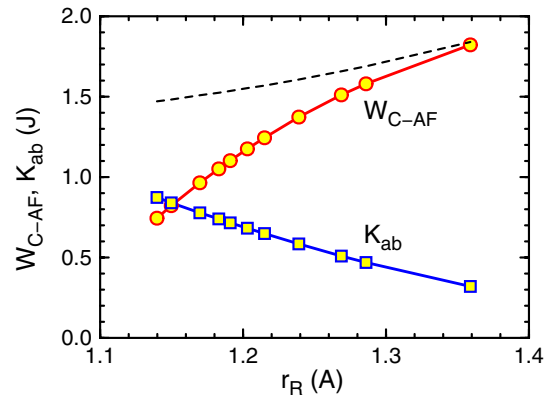

FIG. 4 (color online). The width of magnon band $W_{C\text{-AF}}$ for finite g_{eff} (circles) and without orbital-strain coupling ($g_{\text{eff}} = 0$, dashed line), and orbital interactions in ab planes K_{ab} (squares) in the C-AF phase of cubic vanadates (the points correspond to the RVO$_3$ compounds of Fig. 1). Parameters as in Fig. 2.
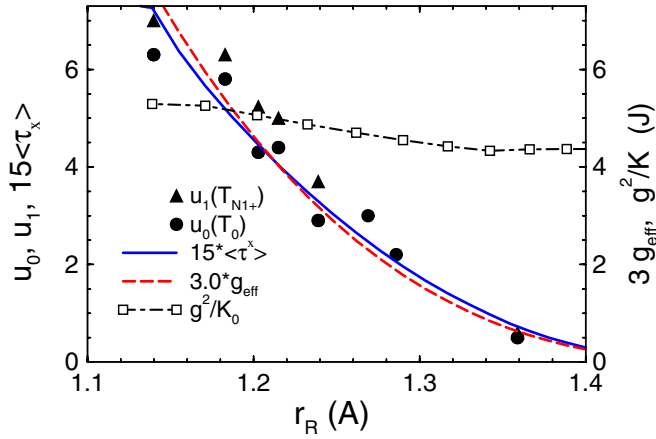
FIG. 5 (color online). Experimental distortion (in percent) at $T_0 = 0$ (u_0, circles) and above T_{N1} (u_1, triangles) for LaVO$_3$ [20] and other RVO$_3$ compounds [19,22], compared with the orbital polarization $\langle \tau^x \rangle_{T=0}$ and with g_{eff} (5); g_{eff} and g^2/K are in units of J. Squares show the upper bound for g^2/K predicted by the theory (at $u_0 = 0$). Parameters as in Fig. 2.

data for the distortion at zero temperature (u_0) and above the first magnetic transition (u_1) exhibit nearly the same dependence on r_R as either the orbital polarization $\langle \tau^x \rangle$, or the effective interaction g_{eff}. This is an unexpected outcome of the present theory as information about the actual lattice distortions has not been used in constructing the spin-orbital model (1), and implies that (i) the full ϑ dependence of g_{eff} is due to $u(\vartheta)$, and the bare coupling parameters $\{g, K\}$ are nearly constant and independent of r_R (Fig. 5), (ii) $g \simeq 33J$ obtained using $u \simeq 0.030 g_{\text{eff}}/J$ (i.e., $g/a_0 \simeq 0.15$ eV/Å for $a_0 = 3.8$ Å), (iii) $\langle \tau^x \rangle = \chi(\vartheta; T) g_{\text{eff}}(\vartheta)$, where the susceptibility $\chi \simeq 0.2/J$ hardly depends on ϑ and only weakly on T (cf. Fig. 3), so that $u(\vartheta) \simeq u_0(\vartheta)/[1 - \chi(T) g^2/K]$, which justifies *a posteriori* our approach with a single parameter g_{eff} (5), depending only on ϑ, and (iv) $K > 220J$ (as $\chi g^2/K < 1$). K may be estimated from the shear modulus which is, however, unknown for RVO$_3$. Taking the data for SrTiO$_3$ [27] instead would imply $K \simeq 6600J$ (i.e., $K/a_0^2 \simeq 8$ eV/Å^2), i.e., a 3%–5% contribution of $\langle \tau^x \rangle$ to u in g_{eff}.

Finally, we emphasize that the experimental data of Fig. 1 are reproduced with rather realistic parameters — taking $J = 202$ K one finds $T_{N1} = 0.73J = 147$ K for LaVO$_3$ ($T_{N1}^{\text{exp}} = 143$ K [2]). Although the present theory brings us closer to the ultimate understanding of the complex phase diagram of the vanadates, several issues remain open. One of them is the second phase transition at T_{N2} to the G-AF phase, which occurs for small r_R [2]. As shown in Ref. [8], this transition is due to an interplay between superexchange orbital fluctuations and orbital-lattice interactions. While this physics is contained in the model (1), its

quantitative description including the recent observations of coexistence of the G-AF and C-AF order [21,22] will have to be addressed in future work.

Summarizing, we have introduced a microscopic spin-orbital model that provides a satisfactory description of the systematic trends for both orbital and magnetic transitions in the RVO$_3$ perovskites, including the nonmonotonic behavior of the OO temperature T_{OO}. Thereby the orthorhombic lattice distortion u, which increases from La to Y by 1 order of magnitude, plays a crucial role — it modifies orbital fluctuations and in this way tunes the onset of both orbital and spin order in the cubic vanadates.

[1] J.-S. Zhou and J. B. Goodenough, Phys. Rev. Lett. **96,** 247202 (2006).
[2] S. Miyasaka *et al.*, Phys. Rev. B **68,** 100406 (2003).
[3] S. Miyasaka *et al.*, Phys. Rev. B **73,** 224436 (2006).
[4] In the G-type phase the order parameter is staggered in all directions, while in the C-type phase it is staggered in the ab planes but remains uniform along the c axis.
[5] C. Ulrich *et al.*, Phys. Rev. Lett. **91,** 257202 (2003).
[6] S. Miyasaka *et al.*, Phys. Rev. Lett. **94,** 076405 (2005).
[7] M. De Raychaudhury, E. Pavarini, and O. K. Andersen, Phys. Rev. Lett. **99,** 126402 (2007).
[8] G. Khaliullin *et al.*, Phys. Rev. Lett. **86,** 3879 (2001).
[9] A. M. Oleś *et al.*, Phys. Rev. B **75,** 184434 (2007).
[10] P. Horsch *et al.*, Phys. Rev. Lett. **91,** 257203 (2003).
[11] J.-S. Zhou *et al.*, Phys. Rev. Lett. **99,** 156401 (2007).
[12] J.-Q. Yan *et al.*, Phys. Rev. Lett. **99,** 197201 (2007).
[13] J.-Q. Yan *et al.*, Phys. Rev. Lett. **93,** 235901 (2004).
[14] M. Mochizuki and M. Imada, New J. Phys. **6,** 154 (2004).
[15] E. Pavarini *et al.*, New J. Phys. **7,** 188 (2005).
[16] J.-S. Zhou and J. B. Goodenough, Phys. Rev. Lett. **94,** 065501 (2005).
[17] The orbital interaction $\mathcal{K}_{ij}$ overestimates the stability of the G-type OO in LaVO$_3$ in the cluster approach.
[18] The data for Ce were not included as the mixed-valent electronic structure of CeVO$_3$ requires a separate study.
[19] M. Reehuis *et al.*, Phys. Rev. B **73,** 094440 (2006).
[20] Y. Ren *et al.*, Phys. Rev. B **67,** 014107 (2003).
[21] M. H. Sage *et al.*, Phys. Rev. Lett. **96,** 036401 (2006).
[22] M. H. Sage *et al.*, Phys. Rev. B **76,** 195102 (2007).
[23] L. F. Feiner and A. M. Oleś, Phys. Rev. B **59,** 3295 (1999).
[24] T. N. De Silva *et al.*, Phys. Rev. B **68,** 184402 (2003).
[25] Orbital correlations along the c axis were renormalized to the disordered orbital chain in LaVO$_3$, $\langle \vec{\tau}_i \cdot \vec{\tau}_j \rangle = \frac{1}{4} - \ln 2$.
[26] The larger or smaller orbital moments $|\langle \tau_i^z \rangle|$ alternate along the c axis in the G-OO phase below T_{OO}.
[27] M. A. Carpenter, Am. Mineral. **92,** 309 (2007).